INTERNATIONAL ATOMIC ENERGY AGENCY
UNITED NATIONS EDUCATIONAL, SCIENTIFIC AND CULTURAL ORGANIZATION
INTERNATIONAL CENTRE FOR THEORETICAL PHYSICS
I.C.T.P., P.O. BOX 586, 34100 TRIESTE, ITALY, CABLE: CENTRATOM TRIESTE

SMR.703 - 23

WORKING PARTY ON
MECHANICAL PROPERTIES OF INTERFACES

23 AUGUST - 3 SEPTEMBER 1993

"High Resolution Electronmicroscope Studies on Interfaces" (Part II)

"Interface and Ductility/Toughness of TiAl"

Heng-Qiang YE
Institute of Metal Research
Academia Sinica
Wenhua Road 72
Shenyang 110015
People's Republic of China

The study of interfaces between TiAl and Ti_3Al phases in the intermetallic compound $Ti_{50.7}Al_{48}Mn_{1.3}$

By L. L. He, H. Q. Ye, X. G. Ning, M. Z. Cao and D. Han

Laboratory of Atomic Imaging of Solids, Institute of Metal Research, Academia Sinica, 72 Wenhua Road, Shenyang 110015, P.R. China

[*Received 1 June 1992*† *and accepted 18 November 1992*]

ABSTRACT

The TiAl(Mn) alloy with lamellar structure of the α_2- and γ-phases is of superior mechanical property in comparison with single α_2- and γ-phases because the α_2–γ and γ–γ interfaces play an important role in improving the ductility. In order to understand their growuh mechanism and the deformation behaviour of the lamellar structure, the fine structures of α_2–γ and γ–γ interfaces were investigated on the atomic scale using transmission electron microscopy and high-resolution electron microscopy. The hierarchy of lamellar structures was firstly detected on the nanometre scale. Some boundaries, stacking faults and dislocations were found in the γ stripes. There are also some twins in which the $[111]_M$–$[11\bar{1}]_T$ directions are not parallel accurately and have 2° deviation between them because of their tetragonality. Two atomic structure models of the α_2–γ interface were suggested and the perfect α_2–γ interface is actually a mixture of these two models. There are also some dislocation ledges and stain concentration at the α_2–γ interface and these ledges are arranged on the interface at regular distance. In the composite interfaces, the γ–γ interfaces show a twin relationship and no α_2 slice between them. A new kind of α_2–γ_B–γ_A–γ_B–α_2 interface was also found. The formation of this composite interface was deduced to be transformed from the α_2–γ_B–γ_B–α_2 interface.

§ 1. Introduction

Nearly equiatomic Ti-rich titanium aluminides are currently being investigated for use as high-temperature materials in aerospace application because they exhibit a desirable combination of high modules retention, creep and oxidation resistance at elevated temperatures, as well as low density (Lipsitt, Shechtman and Schafrik 1975, Lipsitt 1985). They show very limited ductility and toughness below 600°C and can be improved by alloying in a little Mn (Hanamura and Tanino 1989). These alloys are usually composed of a lamellar mixture of TiAl (γ-phase) and Ti_3Al (α_2-phase) and always exhibit superior mechanical properties in comparison with the single TiAl or Ti_3Al phases (Sastry and Lipsitt 1977, Kawabta, Tabano and Izumi 1988). The main reason is that the interfaces between the γ- and α_2-phases play an important role in improving the ductility and toughness. Therefore the study on the interfaces between the α_2- and γ-phases has become more attractive to all researchers who wish to improve the mechanical properties of these high-temperature intermetallic compounds.

In these alloys the γ- and α_2-phases usually form the lamellar structure and have the orientation relationship $\{111\}_\gamma /\!/ (0001)_{\alpha_2}$ and $\langle 110\rangle_\gamma /\!/ \langle 11\bar{2}0\rangle_{\alpha_2}$ (Shechtman, Blackburn and Lipsitt 1974, Williams 1978). The interfaces between the γ- and α_2-phases are the main structures that take collective and concordant action in the deformation

† Received in final form 10 November 1992.

process. These lamellar structures are generated usually through three kinds of phase transformation as follows.

(1) The eutectoid reaction takes place at about 1120°C in the Ti–Al alloy with about 43 at.% Al. The disordered high-temperature α-Ti transforms to the ordered α_2- and γ-phases which construct the lamellar structure (Valencia, McCullough, Levi and Mehrabian 1987). Because this reaction is fulfilled by the long-range diffusion between adjacent slices, the lamellar structure should have characteristics of the alternate arrangement of the γ- and α_2-phases, which means that most of interfaces are γ–α_2 interfaces.

(2) The γ-phase is precipitated from the α_2-phase. The γ-phase can grow from an α_2-phase matrix at dislocations and grain boundaries when isothermal ageing at a suitable temperature in the $\alpha_2+\gamma$ two-phase field in the Ti–Al alloy with 28–38 at.% Al (Blackburn 1970). Such a structural transformation can occur if $(a/6)\langle 10\bar{1}0\rangle$ Shockley partial dislocations traverse every alternate basal plane of the α_2-phase (i.e. stacking faults are introduced). In this case, of course, the long-range atomic transport has to occur through the movement of the dislocation so that the composition and the order states pertinent to the two phases can be attained (Mukhopadhyay 1979).

(3) The α_2-phase can be precipitated from the γ-phase. During isothermal ageing at a suitable temperature below the eutectoid point, the plate-like α_2-phase can be formed from the γ-phase matrix by the migration of the 90° and 30° Shockley partial dislocation ledges with Burgers vector $(a/6\langle 112\rangle$ on alternate $(111)_\gamma$ basal planes pf the γ-phase and the atomic redistribution can be fulfilled by long-range transformation during the movement of the dislocation core (Mahon and Howe 1990). This transformation is very similar to the precipitation of γ′ plates from the disorder α_2 matrix in Ag–Al alloy (Howe 1987), but such α_2 plates should have a limiting size and cannot sometimes form the lamellae structure. In the current studies on the γ–α_2 interface the difference between them has not yet been considered and some confusion exists in describing the interfaces. It is reasonable to believe that there must be some difference between the micromorphologies of the lamellar structures and between the fine atomic structures of the interface between the α_2- and γ-phases, which may also have different effect upon the mechanical properties of the Ti–Al alloy.

The interfaces between the α_2- and γ-phases have been systematically studied using electron diffraction analysis. In addition to the twin structure in the γ-phase, four (or six) kinds of interface between the different γ variants (i.e. with different orientations according to the α_2-phase) were also analysed: these are called twin relationships (Feng, Michel and Crowe 1988, 1989, Schwarta and Sastry 1989, Yang and Wu 1990). The electron diffraction and diffraction contrast analysis, however, are somewhat limited in the study of the fine structures of interfaces. Therefore a high-resolution electron microscopy (HREM) investigation on the atomic scale is needed for the fine structure of interfaces. Mahon and Howe (1990) have observed some dislocation ledges and strain concentration at the α_2–γ interfaces. The twin interfaces and twin relationship are also observed (Mahon and Howe 1990, Inui, Nakamura, Oh and Yamaguchi 1991). However, the system of lamellar structures which have different features has not as yet been very clear. The atomic structure of the γ–α_2 and γ–γ interfaces and the composition transition in the interface region are not understood thoroughly. In this

paper, a study on the fine structure of the interfaces of the α_2- and γ-phases on an atomic scale with HREM observations is reported.

§2. Experimental details

The alloys used in this study were prepared by melting the pure elements Ti, Al and Mn in the proportions 64 wt% Ti, 34 wt% Al and 2 wt% Mn in an Ar atmosphere in a non-consumable arc furnace. The alloys were remelted at least four times in order to achieve homogenization and then cast into rods of diameter 10 mm. The samples for heat treatment were cut from these alloys and encapsulated in a quartz tube back-filled with Ar at $(2–3) \times 10^4$ Pa. The samples in quartz were firstly heated for 2 h at 1250°C to obtain a solution and cooled to room temperature in air, they were then heated for 4 h at 900°C for isothermal ageing and cooled to room temperature again in air. The foils for transmission electron microscopy were prepared by cutting them to 0·2 mm slices with a spark saw and electropolishing them in a twin-jet machine using a 5% $HClO_4$–ethanol electrolyte with about 5 ml of hydrofluoric acid at −30°C and 30 V.

The films were examined in a JEM-200CX electron microscope for electron diffraction and diffraction contrast analysis. The HREM observations on the interfaces of the α_2- and γ-phases along the $[11\bar{2}0]_{\alpha_2}$ direction were carried out using a JEOL-2000EXII high-resolution electron microscope at 200 kV with a resolution power about 0·21 nm.

The computer simulations of HREM images were calculated using a multislice program. The microscope parameters used in the simulations were the spherical aberration coefficient $C_s = 0{\cdot}7$ mm, the defocus spread $\Delta = 10{\cdot}0$ nm and the beam convergency $\theta = 0{\cdot}75$ mrad.

§3. The structure of the γ- and α_2-phases and their calculated HREM images viewed along $\langle 110\rangle_\gamma$ and $\langle 11\bar{2}0\rangle_{\alpha_2}$

The γ-phase has a f.c.t. lattice with an $L1_0$-type structure (AuCuI type) and space group $P4/mmm$. Its lattice parameters are $a = 0{\cdot}397–0{\cdot}401$ nm and $c = 0{\cdot}404–0{\cdot}406$ nm, varying with alloy composition from 49 to 66 at.% Al. The α_2-phase has a hexagonal lattice with a $D0_{19}$-type structure (Sn_3Ni type) and space group $P6/mmc$. Its lattice paraemeters are $a = 0{\cdot}572–0{\cdot}576$ nm and $c = 0{\cdot}460–0{\cdot}464$ nm, varying with the composition from 20 to 38 at.% Al. In the lamellar structure, the γ- and α_2-phases have the orientation relationship $\{111\}_\gamma /\!/ (0001)_{\alpha_2}$ and $\langle 110\rangle_\gamma /\!/ \langle 11\bar{2}0\rangle_{\alpha_2}$. Because the γ-phase is an ordered phase, the $[110]_\gamma$ direction is not equivalent to the $[101]_\gamma$ and $[011]_\gamma$ directions. On the other hand, all $\langle 11\bar{2}0\rangle$ directions of the α_2-phase are equivalent. Therefore the γ-phase should have six possible $\langle 110\rangle_\gamma$ variants with respect to $\langle 11\bar{2}0\rangle_{\alpha_2}$, namely the γ_A, γ_B, γ_C, γ_D, γ_E and γ_F variants respectively. Of these the variants γ_A, γ_C and γ_E are of twin relationship (pseudo-twins) with variants γ_B, γ_D and γ_F. However, only four kinds of variant, namely γ_A, γ_B, γ_C and γ_D can be distinguished in the selected-area electron diffraction (SAED) patterns because the variants γ_C and γ_E, and the variants γ_D and γ_F, are of the same SAED configuration (Yang and Wu 1989).

A series of the image simulation and the experimental observation proved that the different γ variants can also be distinguished in the HREM image. Figure 1 shows the projected structures of the γ- and α_2-phases along the $\langle 110\rangle_\gamma$ and $\langle 11\bar{2}0\rangle_{\alpha_2}$ directions respectively. Figure 1 (*a*) give the $\langle 110]_\gamma$ projection for γ_A and γ_B ($\gamma_{A/B}$), figure 1 (*b*) the $\langle 011]_\gamma$ projection for γ_C and γ_D ($\gamma_{C/D}$), and fig. 1 (*c*) is the α_2-phase along the $\langle 11\bar{2}0\rangle$ direction. In the $\gamma_{A/B}$ variants, there are two kinds of atomic row, namely a pure Ti atom row and a pure Al atom row. They occupy the corner and centre positions respectively

Fig. 1

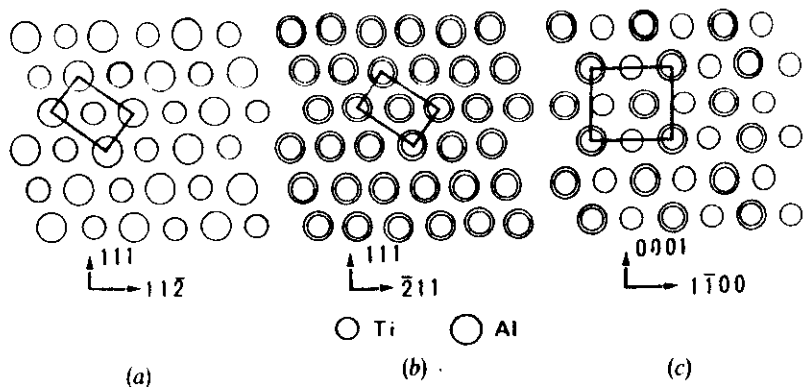

(*a*) (*b*) (*c*)

Projected structures of the γ- and α_2-phases along the $\langle 110\rangle_\gamma$ and $\langle 11\bar{2}0\rangle_{\alpha_2}$ directions respectively.

of the rectangular net. In the $\gamma_{C/D}$ variants there is only one kind of mixed atom rows. Therefore the HREM images of $\gamma_{A/B}$ and $\gamma_{C/D}$ variants should have different configurations. Figure 2 shows the simulated images of the γ-phase viewed along the $\langle 110]_\gamma$ and $\langle 011]_\gamma$ directions, that is the $\gamma_{A/B}$ and $\gamma_{C/D}$ variants, and the images of the α_2-phase along the $\langle 11\bar{2}0\rangle$ direction. The defocus values are 51 nm in fig. 2 (*a*) and 78 nm in fig. 2 (*b*). According to the calculated images, the bright spots sometimes represent the atom rows and sometimes the channels between the atom rows, depending on the thickness and defocus values. The $\gamma_{A/B}$ variant shows that the centred rectangular configuration and the brightness of the spots in corner and centre is different when the samples are much thinner. When their thickness is greater, the $\gamma_{A/B}$ variant appeared to be the rectangular configuration without a centre in which the bright spots represent the pure Ti or pure Al atom rows or the channels, depending on the thickness. The HREM images of the $\gamma_{C/D}$ variants always have the centred rectangular network in which the bright dots are of the same brightness all the time and appear to be the same as that of the disordered f.c.t. structure. The bright dots do not always represent the mixed Ti–Al atom rows, and they represent the channels in a certain thickness. As for the $[11\bar{2}0]$ HREM images of the α_2-phase, when the sample is thinner the Ti and Ti–Al atom rows give rise to bright spots but their brightnesses are different (see the case when $t = 2{\cdot}3$ nm, $\Delta f = 78$ nm, in fig. 2 (*b*)). If the samples are much thinner, the Ti and Ti–Al atom rows mostly show the same brightness. When the film is thicker, only the mixed Ti–Al (or pure Ti) atom rows give rise to the bright spots. The images under the defocus values of 51 and 78 nm are mostly similar for the image dot configuration but the contrast may be reversed. Figure 3 is a typical experimental HREM image viewed along the $[11\bar{2}0]_{\alpha_2}$ direction taken near the edge of a film. The images of γ stripes along the $\langle 110]$ and $\langle 011]$ directions and the α_2-phase stripe along the $\langle 11\bar{2}0\rangle$ direction are demonstrated clearly. In the very thinnest regions the configurations of the different γ variants are the same but in the $_{A/B}$ stripe the brightnesses between the spots at the centre and corner of the rectangle are slightly different. However, they have different configurations in the thicker region, that is $\gamma_{A/B}$ has the rectangular configuration without a centre but $\gamma_{C/D}$ has a centred rectangular configuration. They are mostly according with the calculated image.

Fig. 2

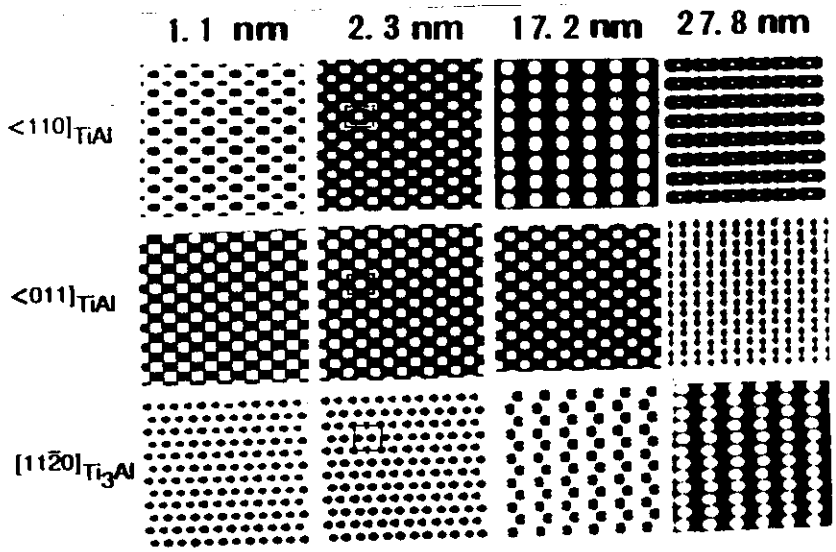

(*a*)

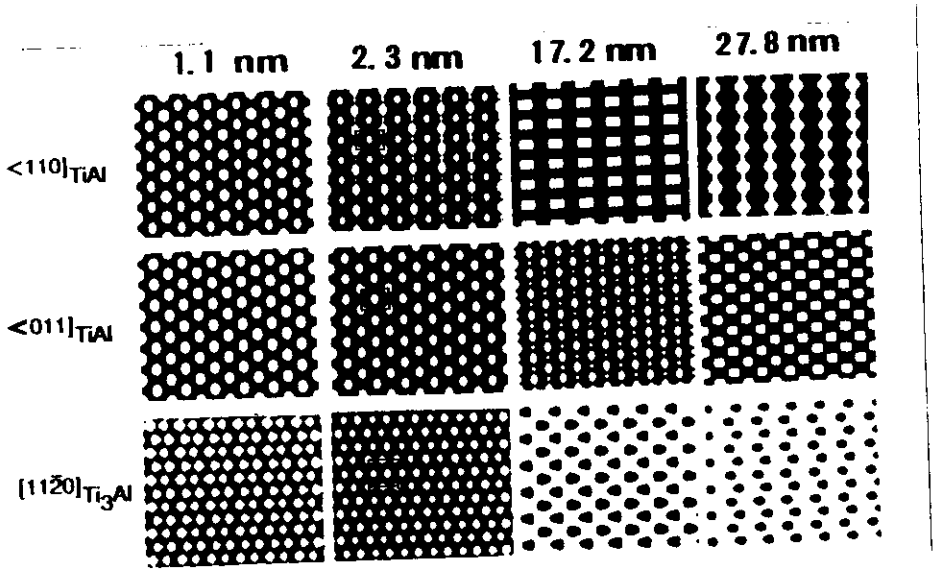

(*b*)

Calculated images of (*a*) the γ-phase viewed along the $\langle 110]_\gamma$ and $\langle 011]_\gamma$ directions, that is the $\gamma_{A/B}$ and $\gamma_{C/D}$ variants, and (*b*) the α_2-phase along the $\langle 11\bar{2}0\rangle$ direction. The defocus values are 51 nm in (*a*) and 78 nm in (*b*).

Fig. 3

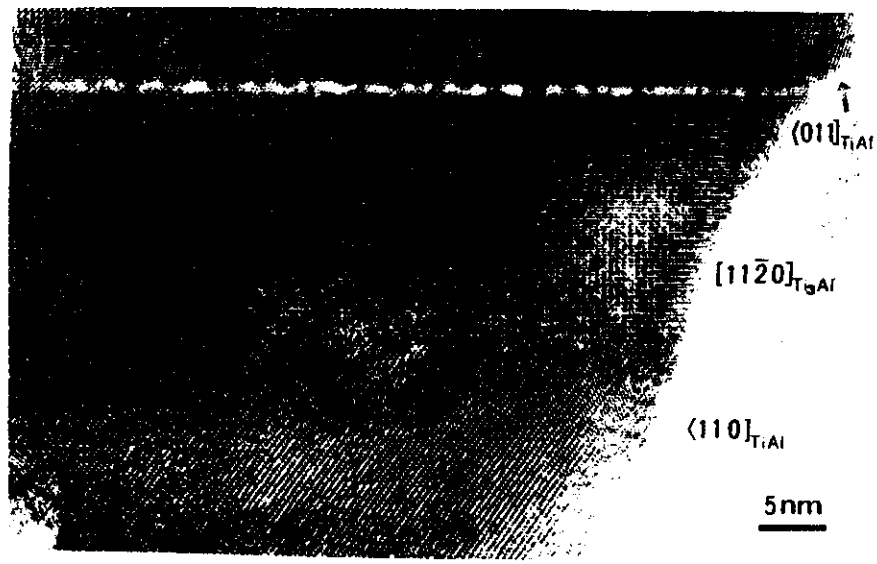

Typical experimental HREM imag. of the γ-α_2 lamellar structure viewed along the $[11\bar{2}0]_{\alpha_2}$ direction taken near the edge of a film.

In summary, the variants γ_A, γ_B, γ_C and γ_D and their orientation relationships with the α_2-phase can be identified by the spot configuration in HREM images. However, in HREM images, γ_E and γ_C, or γ_F and γ_D, cannot be distinguished between.

It is necessary to distinguish between the $\gamma_{A/B}$ and $\gamma_{C/D}$ variants for construction of the atomic models of interfaces of the γ- and α_2-phases because the features of the atom rows at interfaces are different between the α_2–γ_A (or α_2–γ_B) interface and the α_2–γ_C (or α_2–γ_D) interface. For example, the α_2–γ interface showed in fig. 6 in the paper by Mahon and Howe (1990) should be the α_2–γ_C (or α_2–γ_D) interface but the corresponding atomic structure model in their fig. 7 gave rise to the atomic model of the α_2–γ_A (or α_2–γ_B) interface. In the paper by Inui *et al.* (1991) the simulated image in fig. 1 (*d*) is very different from the experimental image in their fig. 2 (*a*) and fig. 3 (*d*), and especially from fig. 3 (*f*). They are actually two kinds of configuration of the $\gamma_{A/B}$ variants in different thicknesses. Therefore accurately identifying the different γ variants is the basis of studying the fine structures of interfaces in these intermetallic compounds.

§4. Results and discussion

4.1. *The hierarchy of lamellar mixture structures*

In this alloy, in addition to some equiaxial γ-phases, most grains show a mixed lamellar structure (fig. 4). There are two kinds of stripes: the bright stripes, denoted S, about 1 μm wide, and the dark stripes, denoted M, about 0·1–0·3 μm wide. The electron diffraction analysis proved that the S stripes are plain γ-phase and the M stripes (actually a region) are a mixture of thinner stripes of α_2-phase and different γ variants. Figures 5 (*a*) and (*b*) are their corresponding SAED patterns, where fig. 5 (*a*) is the SAED pattern from one S stripe and fig. 5 (*b*) shows a composite pattern of $\langle 110 \rangle$ zones

Fig. 4

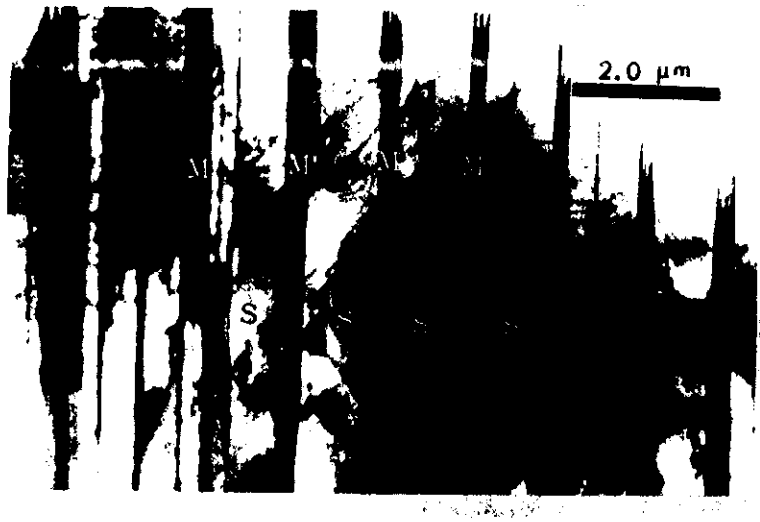

Bright-field image shows the first level of a lamellar structure.

Fig. 5

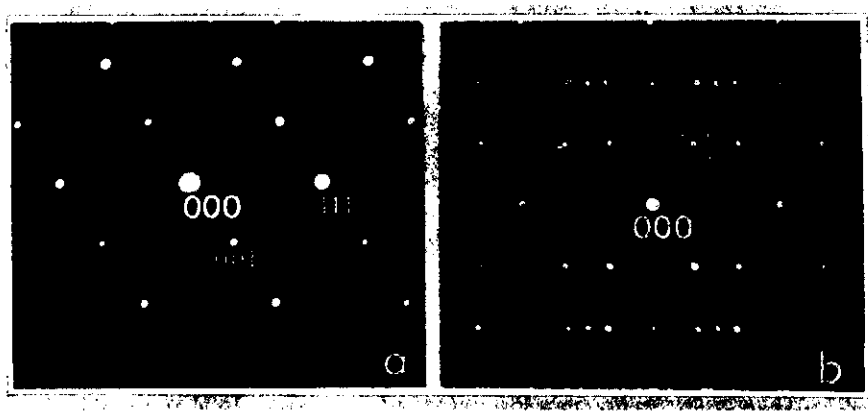

Corresponding SAED patterns taken from the (*a*) S and (*b*) M regions in the fig. 4, respectively.

of the γ-phase and $[11\bar{2}0]$ zone of the α_2-phase. Figure 6 is the $[11\bar{2}0]_{\alpha_2}$ HREM image taken from an M region. The arrangements of α_2-phase and different γ variants along the $[0001]_{\alpha_2}$ or $[111]_\gamma$ direction are demonstrated clearly. The width of these thinner stripes varied from 10 to 30 nm and the α_2 stripes are mostly wider than the γ stripes. This kind of mixed lamellar structure consists of two levels of lamellar structures: a coarse level (S + M) and a fine level ($\alpha_2 + \gamma$ in M). We may call this as a composite lamellar structure or a system of lamellar structures. This hierarchy of lamellar structures is firstly observed on a nanometre scale in this alloy.

The formation of this composite lamellar structure is closely related to the heat treatment process. After first cooling from the 1250°C, only the eutectoid reaction took

Fig. 6

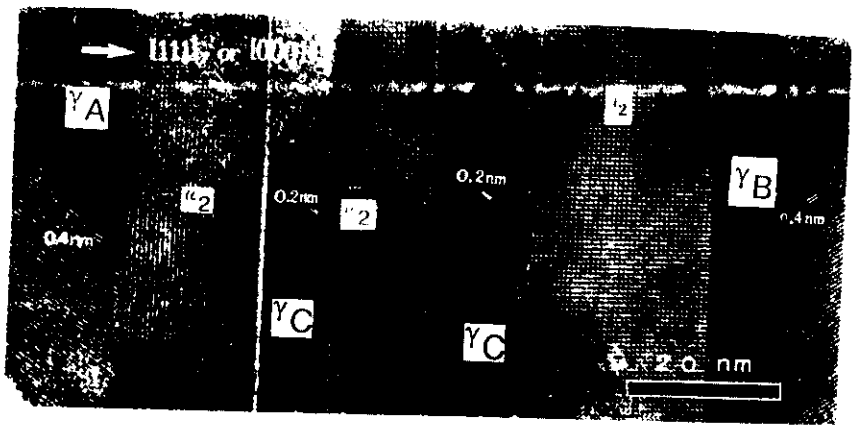

$[11\bar{2}0]_{\alpha_2}$ HREM image taken from an M region shows that the second level of the lamellar structure is composed of α_2 stripes and different γ variants.

place and most of M regions were just the α_2-phase, which meant that only the coarse lamellar structures were formed. On isothermally ageing at 900°C the fine γ stripes precipitated from the α_2-phases and the fine lamellar structures were formed in the M region and gave rise to this composite lamellar structure. The average width of the stripes in the fine lamellar structure may be related to the ageing time.

It can be seen that the stripes of α_2- and γ-phases in the fine lamellar structure may appear to be thin enough to have a concordant action in deformation behaviours like multimembranes. The α_2–γ and γ–γ interfaces in these regions should also have collective deformation behaviours; so we call them a composite interface. In the following study we shall be concentrating on the fine structure of these interfaces in the lamellar structure formed during this precipitating process but firstly we shall discuss some defects and twins in the coarse γ-phase.

4.2. *The microsctructure in the coarse γ phase*

Figure 7 shows some defect structures in the single γ-phase stripes (the S region in the fig. 4). Figure 7 (*a*) demonstrates that there are many planar defects in the γ stripes. For example, many boundaries of different γ variants are shown (one of these is indicated by a white arrowhead), and another kind of defect is labelled L. The corresponding HREM image in fig. 7 (*b*) shows that this defect is a stacking fault. Figure 7 (*c*) demonstrates a number of dislocations with the Burgers vector $\frac{1}{2}[110]$. Most of them cross the whole γ-phase from one side to the other (labelled Q). Since they end at the interface, their movement may cause a change in the interfacial structure. Thus, they may be very difficult to move and hence reduce the ductility of this alloy.

In the equiaxial γ-phase, some $(111)[11\bar{2}]$ twins have been detected. The $[1\bar{1}0]$ HREM images shown in fig. 8 demonstrate a twin stripe in the γ matrix about 35 nm wide. Figure 8 (*a*) shows a bird's-eye view of this deformation twin and fig. 8 (*b*) is an enlarged image of the interface between the matrix and twin. By accurate measurement it can be found that the $[111]_M$ and $[111]_T$ directions are not parallel to each other and have an angular deviation of about 2°. The reason is that the *c* axis of the γ-phase is not the same as the *a* axis, that is there is tetragonality of the γ-phase.

Fig. 7

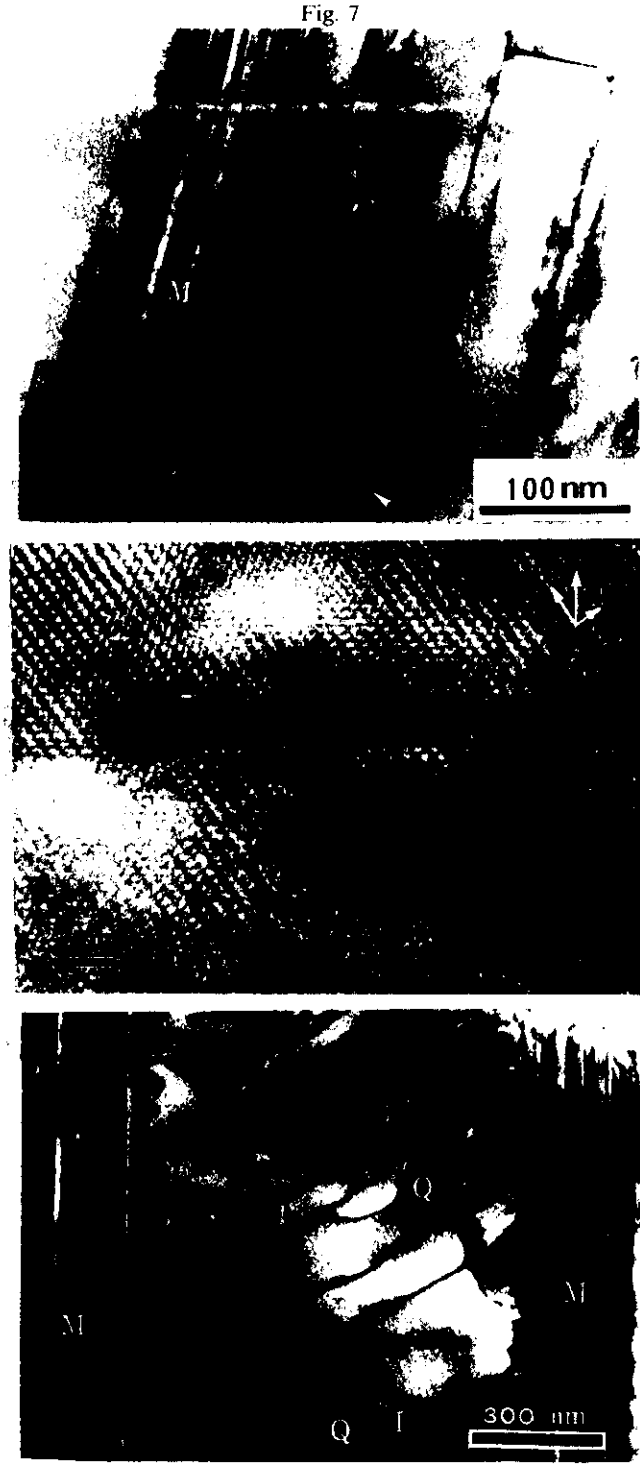

Bright-field image showing (*a*) planar faults and (*c*) dislocations in the single-γ-phase stripes (the S region in fig. 4). The [1$\bar{1}$0] HREM image in (*b*) demonstrates that the defect labelled L is a stacking fault.

Fig. 8

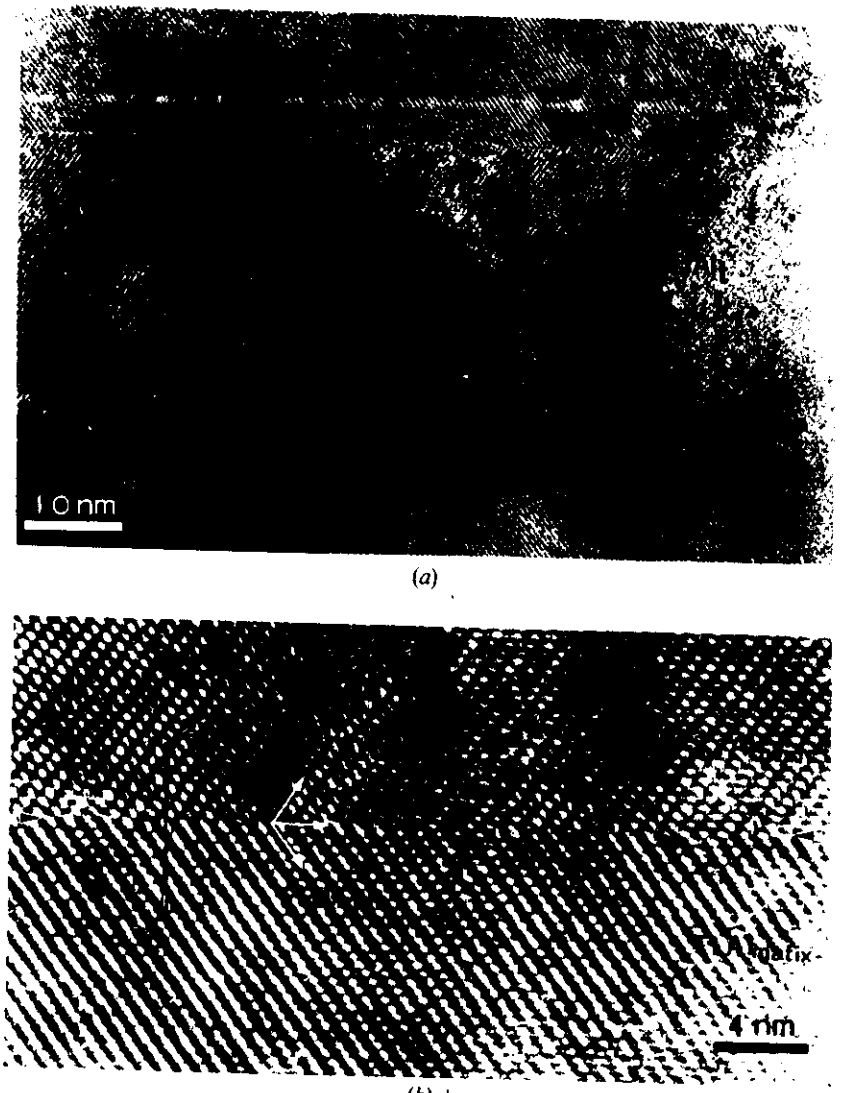

(*a*)

(*b*)

[1$\bar{1}$0] γ twin images demonstrating (*a*) a general view and (*b*) interface detail between the twin variants.

4.3. *The interface between the* α_2- *and* γ-*phases*

Figure 9 is the HREM image observed parallel to the $[01\bar{1}]_\gamma$–$[11\bar{2}0]_{\alpha_2}$ direction which shows a perfect α_2–γ_C interface lying horizontally at the centre. Their corresponding projected cells are respectively outlined in their phase region. The interface is indicated by black arrowheads. The stacking sequences of the α_2- and γ-phases are ABAB and ABCABC and the stacking sequence through the interface is ABABC. At the interface, two kinds of interfacial structure can be detected: an M region and S region. In the S region, the configuration of the spots along the interface 'line' is mostly the same as that in the γ_C variant in which all spots show the same brightness.

Fig. 9

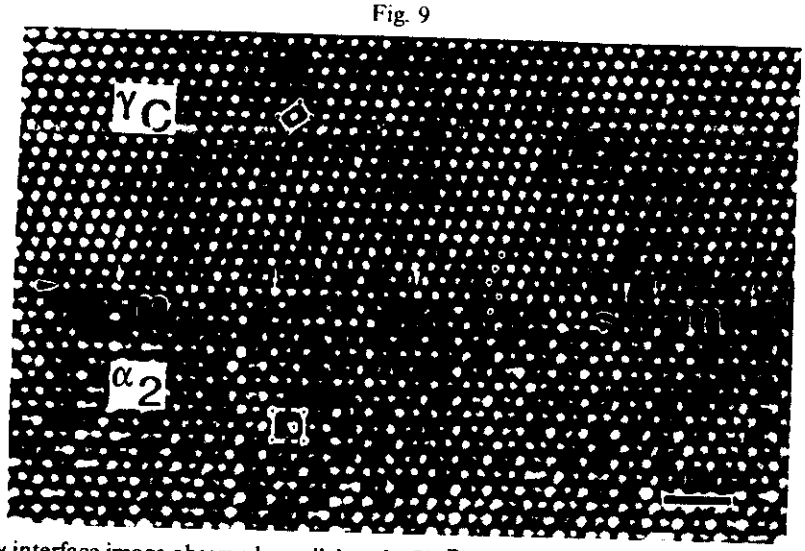

α_2–γ interface image observed parallel to the $[01\bar{1}]^*_{\alpha_2}/[11\bar{2}0]_{\alpha_2}$ direction showing that a perfect α_2–γ_C interface is composed from α_2-like (S) and γ-like (M) interfaces.

This implies that this interface may be composed of mixed Ti–Al atom rows. However, in the M region, the configuration of the spots along the interface 'line' is very similar to that in the α_2-phase in which alternate spots have the same contrast. That is to say this interface is composed of pure Ti atom rows and mixed Ti–Al atoms rows. The former kind of interface is called the γ-like interface and the latter the α_2-like interface. The corresponding atomic structure models are suggested in fig. 10, where fig. 10(*a*) shows the α_2-like interface and fig. 10(*b*) the γ-like interface. Therefore the real α_2–γ interface shown in fig. 9 is actually the mixture interface of α_2-like and γ-like interfaces.

Because of the difference between the lattice parameters of the α_2- and γ-phases the α_2–γ interfaces cannot always remain perfect and some dislocation ledges or strain concentrations often exist at the α_2–γ interfaces. For example, the $[11\bar{2}0]\alpha_2$-$[110]_\gamma$ HREM image in fig. 11 shows a ledge formed at the α_2–γ interface. Because this thinner γ-phase was precipitated from the α_2-phase during isothermal ageing (in the fine lamellar structure region), this ledge can be described as an $(a/6)[1\bar{1}00]$ Shockley partial dislocation in the α_2-phase. Its movement on the $(0001)_{\alpha_2}$ basal plane should cause structure transformation from α_2-phase to γ-phase. Some strain concentration surrounding this dislocation core can be observed. We also observed that these ledges are arranged on the interface at regular distances.

4.4. *Twin relationship in lamellar structures*

When two γ stripes grow from the α_2-phase against each other during the precipitating process, the two γ stripes may meet and form the γ–γ interface. If this γ–γ interface is considered in isolation there are only three kinds of γ–γ interface, namely the γ_A–γ_B, γ_C–γ_D and γ_A–γ_C (or γ_B–γ_D) interface (Inui *et al.* 1991). However, these γ–γ interfaces should be considered according to their relationship with the α_2-phase because they were precipitated from the α_2 matrix. Moreover, they are only 10–30 nm wide and must have a collective or concordant action in the deformation behaviour during macroscopic strain. Thus, they can be considered as a composite interface like a

Fig. 10

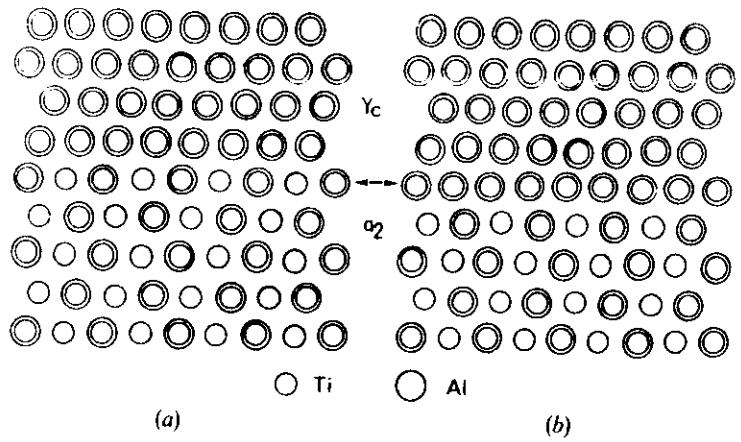

Atomic structure models of the two kinds of α_2–γ interfaces: (*a*) α_2-like interface; (*b*) γ-like interface.

Fig. 11

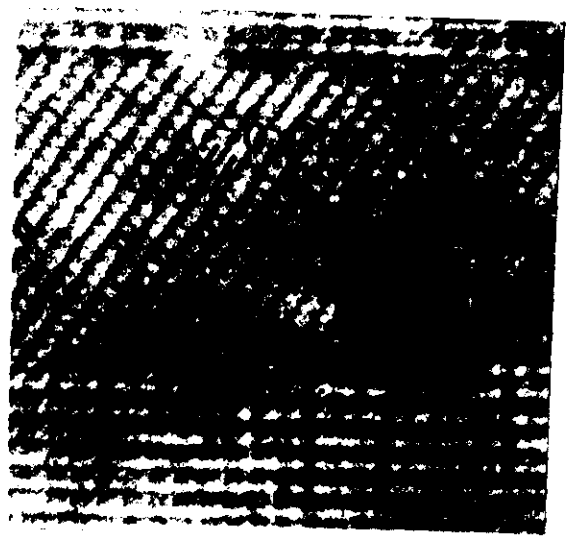

$[11\bar{2}0]_{\alpha_2}$–$[110]_\gamma$ HREM image showing a ledge formed at the α_2–γ interface.

multimembrane. All six γ variants have twin relationships, which can easily be identified from diffraction patterns along the $\langle 11\bar{2}0\rangle_{\alpha_2}$ direction. However, the twin relationship does not always remain perfect in the HREM image of γ–γ variants, and a shift occurs at the γ–γ twin interfaces. Figure 12 shows one kind of these twin relationship in the composite interface α_2–γ_B–γ_A–α_2. At the γ_A–γ_B interface the bright spots are not aligned and a slight shift exists between the two γ variants. The α_2–γ_A interface in the lower region is mostly perfect but the α_2–γ_B interface in upper region is not. Figure 13 shows the α_2–γ_C–γ_D–α_2 composite interface with another kind of twin relationship. The γ_C–γ_D interface is not aligned too. The α_2–γ_C interface in the upper region is perfect but the α_2–γ_D interface in the lower part is not and some strain

Fig. 12

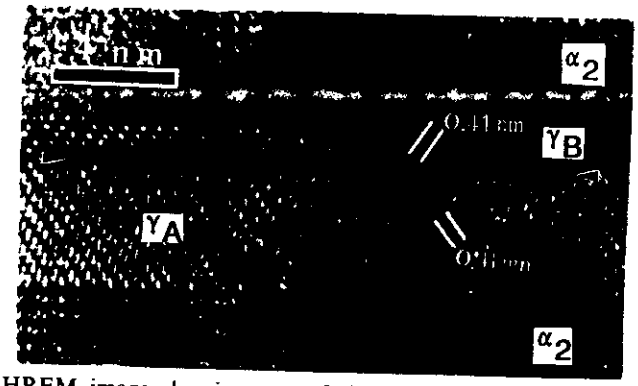

$[11\bar{2}0]_{\alpha_2}$–$[110]_{\gamma}$ HREM image showing one of the twin relationships with the composite interface α_2–γ_B–γ_A–α_2.

Fig. 13

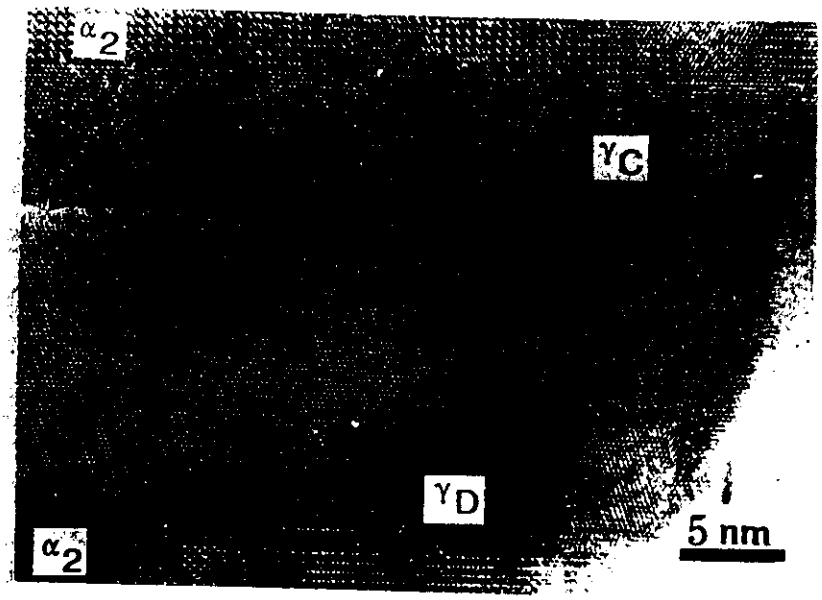

$[11\bar{2}0]_{\alpha_2}$–$[011]_{\gamma}$ HREM image showing the α_2–γ_C–γ_D–α_2 composite interface, which is another kind of twin relationship.

concentration exists. From the above-mentioned HREM images, one may propose a reasonable growth mechanism of the γ stripes from the α_2 matrix. The γ stripes generated from two separated α_2 stripes may meet at a (111) plane with a relative translation. As a result, their relationship is usually 'imperfect'. In these two images it is evident that there is no α_2-phase stripe between the γ_A and γ_B variants or the γ_C and γ_D variants. It is unnecessary for an α_2 slice to exist between the different γ variants according to the formation mechanisms of these γ–γ interfaces.

Fig. 14

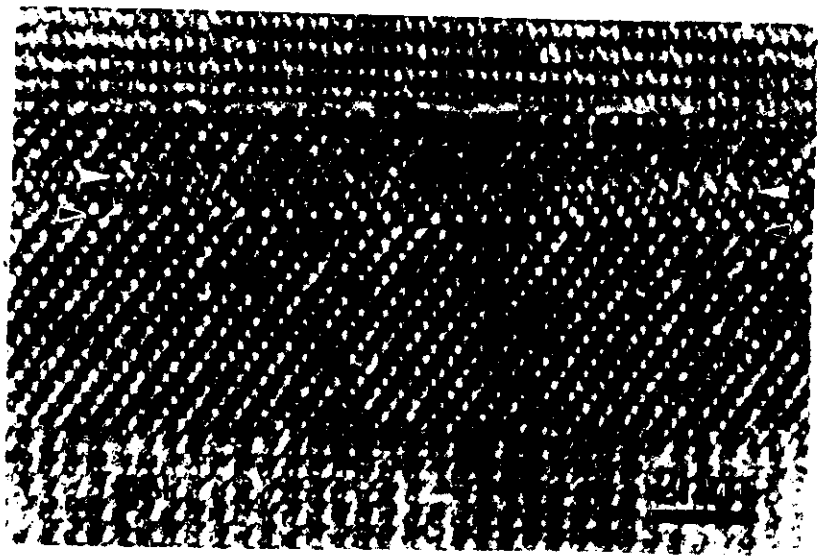

$[11\bar{2}0]_{\alpha_2}$–$[110]_{\gamma}$ HREM image demonstrating the newly found α_2–γ_B–γ_A–γ_B–α_2 composite interface.

Figure 14 demonstrates the characteristic composite interface of the α_2- and γ-phases with the orientational relationship α_2–γ_B–γ_A–γ_B–α_2. The γ_A and the lower γ_B (γ'_B) variants are not aligned evidently but the γ_A and the upper γ_B (γ_B) variants are mostly aligned. This implies that the γ_A and γ_B variants are real twins, and the γ_A and γ'_B variants have a twin relationship only. Hence the formation of these interfaces may be that two γ_B variants grew from the α_2 matrix against each other and they met so as to form the γ_B–γ_B interface without alignment between them. Because this interface is of much higher interfacial mismatch energy, a twin slab is easily formed in one of the variants (in this condition a twin is formed in the γ_B region).

In figs. 12–14 we can detect that the α_2 stripes at top and bottom are aligned, which imply that the two α_2 stripes are actually one α_2-phase matrix. This also proved that the different γ variants in these smaller lamellar structure (in the region in fig. 4) are the phase precipitated from the α_2-phase matrix during ageing at 900°C.

§ 5. Conclusions

(1) The image calculation and the experimental observation proved that four kinds of γ variants, γ_A, γ_B, γ_C and γ_D, can be accurately identified by their configurations and orientation relationships with the α_2-phase in the HREM image. This is the basis of studying the atomic structure of the α_2–γ and γ–γ interfaces.

(2) The lamellar structure may consist of double levels. For example, the lamellar mixture of single-γ-phase stripes about 1 μm wide and lamellar structure 0·1–0·3 μm wide which is composed of thinner stripes of α_2- and γ-phases with width 10–30 nm has been found. The α_2 stripes are usually wider than the γ stripes.

(3) In the single-γ-phase stripes there are many variant boundaries, stacking faults and dislocations. They must affect the mechanical properties.

(4) In the $(111)[11\bar{2}]$ twin the $[111]_M$ and $[111]_T$ directions are not parallel accurately and have 2° deviation between them.

(5) At the α_2–γ interface there are some ledges and strain concentration, which may reduce the mismatch energy caused by the lattice mismatch berween the α_2- and γ-phases. There are two kinds of α_2–γ interfacial structure model: the α_2-like interface and the γ-like interface. The actual α_2–γ interface is composed of the two models.

(6) In the lamellar structure formed by precipitation of the γ-phase from the α_2 matrix there are many composite interfaces with a twin relationship and no α_2 slice is needed inside the γ–γ interface in which two twin-relationship variants sometimes are not perfectly aligned at the interface. Of these composite interfaces a new kind of α_2–γ_B–γ_A–γ_B–α_2 composite interface was found.

Acknowledgment

This work was supported by Grant No. 59291000 from the National Natural Science Foundation of China, which is gratefully acknowledged.

References

Blackburn, M. J., 1970, *The Science, Technology and A--lications of Titanium*, edited by R. Jaffee, and N. E. Promised (Oxford: Pergaman Press), p. 633.

Feng, C. R., Michel, D. J., and Crowe, C. R., 1988, *Scripta metall.*, **22**, 1481; 1989, *Scripta metall.*, **23**, 1136.

Hanamura, T., and Tanino, M., 1989, *J. Mater. Sci. Lett.*, **8**, 24.

Howe, J. M., 1987, *Phil. Mag.* A, **56**, 3561.

Inui, H., Nakamura, A., Oh, M. H., and Yamaguchi, M., 1991, *Ultramicroscopy*, **39**, 268.

Kawabta, T., Tabano, M., and Izumi, O., 1988, *Scripta metall.*, **22**, 1275.

Lipsitt, H. A., 1985, *High-Temperature Ordered Intermetallic Alloys I*, edited by C. C. Koch, C. T. Liu and N. S. Stoleff, Materials Research Society Symposium Proceedings, Vol. 39 (Pittsburgh, Pennsylvania: Materials Research Society), p. 351.

Lipsitt, H. A., Shechtman, D., and Schafrik, R. E., 1975, *Metall. Trans.* A, **6**, 1991.

Mahon, G. J., and Howe, J. M., 1990, *Metall. Trans.* A, **21**, 1655.

Mukhopadhyay, P., 1979, *Metallography*, **12**, 119.

Sastry, S. M. L., and Lipsitt, H. A., 1977, *Metall. Trans.* A, **8**, 299.

Schwartz, D. S., and Sastry, S. M. L., 1989, *Scripta metall.*, **23**, 1621.

Shechtman, D., Blackburn, M. J., and Lipsitt, H. A., 1974, *Metall. Trans.*, **5**, 1373.

Valencia, J. J., McCullough, C., Levi, C. G., and Mehrabran, R., 1987, *Scripta metall.*, **21**, 1341.

Williams, J. C., 1978, *Precipitation Processes in Solids* edited by K. C. Russell and H. I. Aronson (Warrendale, Pennsylvania: Metallurgical Society of AIME), p. 191.

Yang, Y. S., and Wu, S. K., 1990, *Scripta metall.*, **24**, 1801.